



**EDUARDO LOPES MONTEIRO**

BSc student

# **HYDROGELS FOR LOAD SUPPORT IN THE NUCLEUS PULPOSUS OF INTERVERTEBRAL DISCS**

BACHELOR IN MATERIALS ENGINEERING

NOVA University Lisbon  
June, 2024



# HYDROGELS FOR LOAD SUPPORT IN THE NUCLEUS PULPOSUS OF INTERVERTEBRAL DISCS

**EDUARDO LOPES MONTEIRO**

BSc student

**Adviser:** Susete Nogueira Fernandes

*Assistant Professor, NOVA University Lisbon*

**Co-adviser:** João Paulo Borges

*Full Professor, NOVA University Lisbon*

## Examination Committee

**Chair:** Name of the committee chairperson  
*Full Professor, FCT-NOVA*

**Rapporteur:** Name of a rapporteur  
*Associate Professor, Another University*

**Members:** Another member of the committee  
*Full Professor, Another University*  
Yet another member of the committee  
*Assistant Professor, Another University*

BACHELOR IN MATERIALS ENGINEERING

NOVA University Lisbon

June, 2024

## **Hydrogels for load support in the nucleus pulposus of intervertebral discs**

Copyright © Eduardo Lopes Monteiro, NOVA School of Science and Technology, NOVA University Lisbon.

The NOVA School of Science and Technology and the NOVA University Lisbon have the right, perpetual and without geographical boundaries, to file and publish this dissertation through printed copies reproduced on paper or on digital form, or by any other means known or that may be invented, and to disseminate through scientific repositories and admit its copying and distribution for non-commercial, educational or research purposes, as long as credit is given to the author and editor.



## ACKNOWLEDGEMENTS

This work was supported by FCT-Fundacao para a Ciéncia e a Tecnologia, I.P., in the scope of the project's LA/P/0037/ 2020, UIDP/50025/2020 and UIDB/50025/2020 of the Associate Laboratory Institute of Nanostructures, Nanomodelling and Nano - fabrication-i3N.



## ABSTRACT

Low back pain is one of the most prevalent global health issues, affecting millions of people. It is especially common among adults and is the leading cause of work incapacity worldwide. This condition is often linked to intervertebral disc disease (IDD), which typically begins in the nucleus pulposus (NP). Treatment methods frequently fail to fully restore the intervertebral disc's functions and structure. This project aims to address this problem by developing a thermosensitive injectable hydrogel based on chitosan (CS) and reinforced with cellulose nanocrystalline (CNC) designed to restore the functions and structure of the damaged NP.

Multiple samples of hydrogels with varying concentrations of cellulose nanocrystalline and  $\beta$ -Glycerophosphate (GP) were studied and characterized. The addition of CNCs and GP proved to create a promising system with good gelation temperatures and good mechanical properties. These systems showed Young's modulus values higher than that of a healthy NP, between 9-19 kPa. Along with this, a confined compression system was developed as well to adapt the existing equipment for additional tests of the hydrogels. This development showed its challenges, proving that 3D-printed PLA is not an ideal material for this type of application.

Keywords: Hydrogel; Thermosensitive; CNCs; Chitosan;  $\beta$ -GP; Lactic Acid.



## RESUMO

A dor lombar é um dos problemas de saúde mais prevalentes a nível global, afetando milhões de pessoas. É especialmente comum entre adultos e é a principal causa de incapacidade laboral em todo o mundo. Esta condição está frequentemente associada à doença degenerativa do disco (DDD), que tipicamente começa no núcleo pulposo (NP). Os métodos de tratamento frequentemente falham em restaurar completamente as funções e a estrutura do disco intervertebral. Este projeto visa abordar esse problema desenvolvendo um hidrogel injetável termossensível à base de quitosano (CS) e reforçado com celulose nanocristalina (CNC), projetado para restaurar as funções e a estrutura do NP danificado.

Várias amostras de hidrogéis com diferentes concentrações de celulose nanocristalina e  $\beta$ -glicerofosfato (GP) foram estudadas e caracterizadas. A adição de CNCs e GP mostrou criar um sistema promissor com boas temperaturas de gelificação e boas propriedades mecânicas. Esses sistemas apresentaram valores de módulo de Young superiores aos de um NP saudável, entre 9-19 kPa. Juntamente com isso, foi desenvolvido um sistema de compressão confinada para adaptar o equipamento existente para testes adicionais dos hidrogéis. Este desenvolvimento apresentou desafios, provando que o PLA impresso em 3D não é um material ideal para este tipo de aplicação.

Palavras chave: Hidrogel; Termossensível, CNCs; Quitosano;  $\beta$ -GP; Ácido Lático.



# CONTENTS

|  |            |
|--|------------|
| <b>List of Figures</b>   | <b>xi</b>  |
| <b>List of Tables</b>  | <b>xii</b> |
| <b>1 Introduction</b>  | <b>1</b>   |
| 1.1 Intervertebral Discs and Intervertebral Disc Disease (IDD) . . . . . | 1          |
| 1.2 Objective . . . . .  | 2          |
| 1.3 Hydrogels . . . . .  | 2          |
| 1.3.1 Chitosan . . . . .   | 2          |
| 1.3.2 Cellulose Nanocrystals . . . . .                                   | 2          |
| 1.3.3 $\beta$ -Glycerophosphate . . . . .                                | 3          |
| 1.3.4 Lactic Acid . . . . .  | 3          |
| 1.4 Liquid Crystals . . . . .  | 3          |
| <b>2 LITERATURE REVIEW</b>   | <b>4</b>   |
| <b>3 MATERIALS AND METHODS</b>   | <b>6</b>   |
| 3.1 Materials . . . . .  | 6          |
| 3.2 Preparation of CNC 4.5% Suspension . . . . .                         | 6          |
| 3.3 Preparation of Hydrogel Composite . . . . .                          | 6          |
| 3.4 Hydrogels Production . . . . .                                       | 7          |
| 3.5 Rheology Tests . . . . .   | 7          |
| 3.5.1 Temperature Sweep Test and Viscosity . . . . .                     | 7          |
| 3.6 Unconfined & Confined Compression Tests . . . . .                    | 8          |
| <b>4 RESULTS AND DISCUSSION</b>  | <b>9</b>   |
| 4.1 Designing the Compression System . . . . .                           | 9          |
| 4.2 Rheology Tests . . . . .   | 10         |
| 4.2.1 Temperature Sweep Test . . . . .                                   | 10         |
| 4.2.2 Viscosity . . . . .  | 10         |

|          |   |           |
|----------|---|-----------|
| 4.3      | Preparing Hydrogels . . . . .                       | 11        |
| 4.4      | Compression Tests . . . . .                         | 12        |
| 4.4.1    | Unconfined Tests . . . . .                          | 12        |
| 4.4.2    | Confined Tests . . . . .                            | 13        |
| 4.5      | Additional Tests . . . . .                          | 16        |
| <b>5</b> | <b>Conclusions</b>                                  | <b>19</b> |
|          | <b>Bibliography</b>                                 | <b>21</b> |
|          | <b>Appendices</b>                                   |           |
| <b>A</b> | <b>Development of the Compression System</b>        | <b>24</b> |
| <b>B</b> | <b>CNC suspension 4.5% and gravimetric analysis</b> | <b>26</b> |

## LIST OF FIGURES

|   |    |
|---|----|
| 1.1 Stress comparison of young, old, and degenerated nucleus polpusus . . . . .   | 1  |
| 2.1 Average gelation time and complex modulus of hydrogels; macroscopic view of revised setup highlighting visibility of sample within chamber, and elastic modulus obtained by unconfined compressive mechanical tests . . . . . | 5  |
| 4.1 CAD design . . . . .  | 9  |
| 4.2 Summary of the gelation temperatures obtained from the temperature sweep tests . . . . .  | 10 |
| 4.3 Summary graph of the viscosity curves as a function of the shear rate for the 2% & 3% CNC samples series at 20°C . . . . .  | 11 |
| 4.4 Perspective a) top view and b) front view of a CS/GP9%/CNC2% hydrogel, with a scale bar of 5 mm. . . . .  | 11 |
| 4.5 Stress/strain curve obtained from a compression test of the CS/GP9%/CNC3% sample . . . . .  | 12 |
| 4.6 Histogram of the Young's moduli obtained at 37°C, with n=5 . . . . .  | 13 |
| 4.7 First results from confined compression tests with high noise with sample 2CS/2CNC/9GP . . . . .  | 14 |
| 4.8 Results of compression tests with sample 2CS/2CNC/9GP after surface treatment as done to the system . . . . .   | 15 |
| 4.9 Results of the last compression tests with sample 2CS/2CNC/9GP . . . . .  | 16 |
| 4.10 Confined compression base after 20 tests were performed and cleaned . . . . .  | 16 |
| 4.11 Birefrigence effect observed when sample is seen between crossed polarizers, with a scale bar of 13.7 mm. . . . .  | 17 |
| 4.12 Viscosity as a function of shear rate for aqueous suspensions of CNC with 3.5 and 4.5 wt.% and CNC (4.5 wt.%) with acid lactic. Duplicates are shown to highlight test accuracy . . . . .                                    | 17 |
| A.1 Progress of compression system development. . . . .   | 25 |

## LIST OF TABLES

|  |    |
|--|----|
| 3.1 Composition and gelation times of each composite mixture . . . . . | 7  |
| B.1 Gravimetric analysis of the CNC 4.5% suspension . . . . .          | 26 |

# INTRODUCTION

## 1.1 Intervertebral Discs and Intervertebral Disc Disease (IDD)

The intervertebral disc, composed of the nucleus pulposus (NP) enclosed by the annulus fibrosus (AF), along with the upper and lower cartilage endplates (UCE, LCE), serves as a crucial component of the spine's biomechanics and structural integrity. The NP, characterized by its jelly-like consistency and high water content of up to 90%, is rich in proteoglycans, with small quantities of type II collagen and elastin fibers. The NP provides essential functions, including support, shock absorption, and both facilitation and resistance to excessive movement [2]. While its ability to withstand axial loads is significant, it diminishes with age, contributing to age-related changes in spinal health and function [3]. This degeneration of the Intervertebral disc, also known as Intervertebral disc disease (IDD), is a process marked by various changes, including the loss of water content within the nucleus pulposus [4]. This reduction in hydration levels can lead to alterations in the disc's structure and function, diminishing its ability to effectively cushion and support the spine, as seen in Figure 2.1.

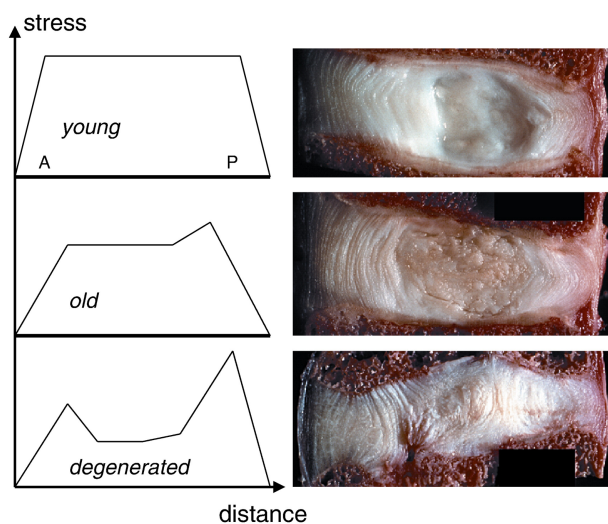


Figure 1.1: Stress comparison of young, old, and degenerated nucleus pulposus. Source: [5]

As the disc degenerates, it becomes more susceptible to wear and tear, contributing to conditions such as herniated discs, spinal stenosis, and osteoarthritis. This degenerative process is frequently cited as one of the leading causes of neck and back pain, as the compromised discs may impinge on nearby nerves or result in instability within the spine, prompting discomfort and functional limitations.

## 1.2 Objective

This work aims to develop a less invasive form of treatment for IDD compared to methods currently used, the most common being spinal fusion [6]. In this study we will attempt to produce a chitosan (CS) based hydrogel reinforced with cellulose nanocrystals (CNCs) that mimics a healthy NP.

## 1.3 Hydrogels

Hydrogels, composed of three-dimensional polymer networks, exhibit a unique combination of properties that make them highly attractive for biomedical applications. Their hydrophilic nature enables them to absorb and retain large quantities of water within their structure, resembling the hydrated environment of biological tissues. Notably, hydrogels demonstrate mechanical characteristics remarkably similar to NP tissue [7]. This resemblance has spurred considerable interest in utilizing hydrogels for the treatment of IDD. For this application, some specific characteristics such as biocompatibility and biodegradability would be required, therefor the following components were selected for the composition of the hydrogels.

### 1.3.1 Chitosan

Chitosan, a biopolymer derived from the deacetylation of chitin, stands as a versatile material with broad applications in both engineering and medical domains. Formed from the structural component of the outer skeletons of crustaceans, insects, and fungal walls, chitin serves as the precursor for chitosan, which comprises D-glucosamine and N-acetyl-D-glucosamine units interconnected in a random arrangement. Its unique properties include being nontoxic, biodegradable, biocompatible, and bio available, making it highly suitable for biomedical and environment applications [8].

### 1.3.2 Cellulose Nanocrystals

Cellulose nanocrystals (CNCs) represent a remarkable class of nano materials derived from cellulose, the primary component of plant cell walls, which can be extracted from various natural sources including wood pulp, cotton, microcrystalline cellulose, and bacterial cellulose. These unique rod-shaped particles possess exceptional properties such as high strength, stiffness, and biodegradability, rendering them highly valuable in a wide range

of applications spanning nanotechnology, materials science, and biomedical engineering [9].

### 1.3.3 $\beta$ -Glycerophosphate

Beta-glycerophosphate (GP) is an organic compound naturally present in the human body, with significant implications in biomedical applications. It is recognized as an osteogenic factor when included in the culture medium of human bone marrow stem cells, promoting their differentiation into bone-forming cells. Additionally,  $\beta$ -glycerophosphate serves as a catalyst in temperature-sensitive hydrogels based on chitosan. In chitosan solutions, at physiological pH and temperatures,  $\beta$ -glycerophosphate facilitates the conversion of fluid to gel phase, enabling the formation of stable hydrogel matrices [10].

### 1.3.4 Lactic Acid

Lactic acid is an organic acid produced primarily during anaerobic metabolism, notably in muscle cells, as a byproduct of glucose metabolism. This acid has the molecular formula CH<sub>3</sub>CH(OH)COOH and is a chiral molecule, existing in the form of L- or D-lactic acid enantiomers [11].

## 1.4 Liquid Crystals

Liquid crystals are a state of matter that presents properties similar to those of conventional liquids as well as to solid crystals. This means that the molecules retain some degree of molecular order but still flow like a liquid. Cellulose nanocrystals show this behavior when suspended in water and above critical concentration. More specifically they self-assemble into a cholesteric liquid crystalline phase, meaning that the nanoparticles are oriented parallel to each other within each pseudo-layer, and overall, the organize into a helical like structure [12].

## LITERATURE REVIEW

Many studies have been conducted in the last few decades to test the effectiveness of hydrogels as a form of cell therapy and treatment for IDD to promote regeneration of the NP [7]. Based on these and the materials presented in the Introduction above, some examples are presented below.

One such example is a study conducted in 2020 by Maturavongsadit et al. to test a CS and CNC hydrogel to promote bone regeneration. The addition of CNCs to the mixture proved to be highly beneficial, with an increase in mechanical strength from 28kPa to 379kPa and an improvement in gelation as shown in Figure 2.1-(a). It was also tested *in vivo* demonstrating significant biocompatibility and high cell viability, proving to be a promising biomaterial for bone regeneration [13].

The authors Kommos et al. designed a new compression setup, to be able to perform confined compression tests, in order to improve accuracy and sample visibility. To achieve these results, a new compression test setup was designed. The major changes to this setup were an increase to surface area and an optically transparent chamber fabricated using SLA printing. These changes to the chamber allowed for a more precise positioning of the samples within the chamber and imaging of the tests. The increase in surface area served to increase the force response during the initial part of testing. These changes can be seen in Figure 2.1-(b). These changes were proven to be effective as a large range of force values could be captured with an improved accuracy resulting in significant differences in force and aggregate modulus measurements. Along with improved mechanical characterization the transparency of the chamber provided real-time monitoring for additional assessment [14].

Thermal-sensitive hydrogels using glycerophosphate are common in biomedicine and have been widely researched. One such study, by Rahamanian-Devin et al., reviews the specific characteristics and possible applications of a chitosan- $\beta$ -glycerophosphate hydrogel. This system has many advantages such as the ability to store large amounts of drug in its network, a controlled rate of release, biodegradability and biocompatibility. With this they concluded this system to be a great substitute for other forms of implants and suitable environment for tissue engineering. Some applications mentioned are spinal

injuries, cell therapy, and certain ocular and respiratory injuries. In addition, it was mentioned that depending on the application additional components can be added to the composition to reach the ideal mechanical and chemical characteristics [8].

A 2018 study by Qin et al. is an example of this. The changes in physical, chemical and biological properties of GO/CS/GP hydrogels were observed with varying GO/CS weight ratios. The results found that all groups had an increase in mechanical properties, including an increase in the Young's modulus of 1.76 to 2.94 times compared to pure CS/GP hydrogels. These results are seen in Figure 2.1-(c). The biocompatibility tests showed great results for the lower content of GO and not so favorable for the higher contents of GO, resulting in the lower contents proving to be better suited for cell attachment with potential for application in tissue engineering. [15]

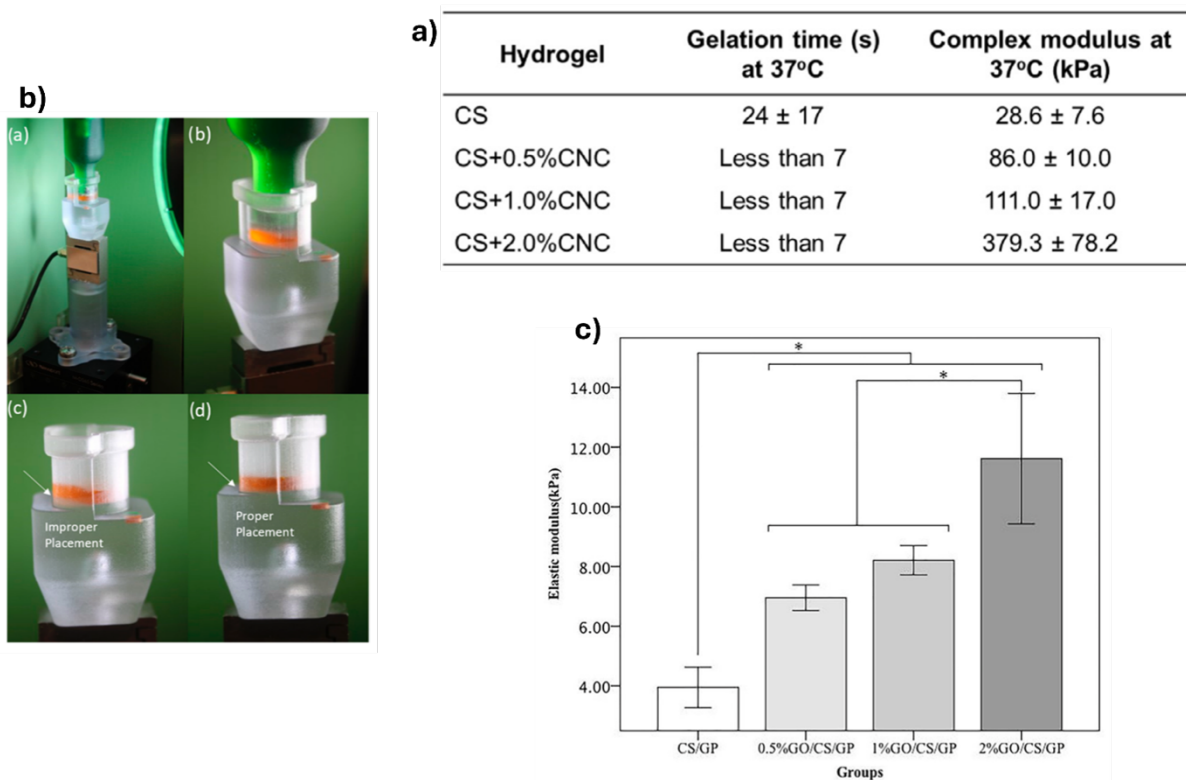


Figure 2.1: a) Average gelation time and complex modulus of hydrogels (source: [13]); b) Macroscopic view of revised setup highlighting visibility of sample within chamber (source: [14]); c) Elastic modulus obtained by unconfined compressive mechanical tests (source: [15]).

# MATERIALS AND METHODS

## 3.1 Materials

The CNC nanofibers, 6.04% solution, were acquired from Celluforce; the chitosan powder, 75.5% deacetylation and molecular weight 469 kDa, obtain from Cognis; the lactic acid 85% solution and disodium  $\beta$ -glycerophosphate hydrate were obtained from Sigma-Aldrich. Ultrapure water type 2, also referred to as millipore ultrapure water, was also used, prepared using an Elix® Advantage 3 Water Purification System.

## 3.2 Preparation of CNC 4.5% Suspension

To prepare a CNC suspension with a concentration of 4.5%, the 6.04% CNC solution was diluted in millipore ultrapure water and sonicated at 153 KJ/g CNCs. It was then filtered through a 50 50  $\mu\text{m}$  filter using an air pump followed by 1,6  $\mu\text{m}$  filter using a syringe. Once filtered it was covered with tinfoil and left to rest.

## 3.3 Preparation of Hydrogel Composite

To make the hydrogel composites, multiple CS/CNC/GP solutions were prepared with different concentrations of CNC and GP, all with a total mass of 50 grams. For these mixtures, the original CNC solution of 6.04% was used and was diluted in millipore ultrapure water to obtain the desired concentrations: 1%, 2%, 3% e 4% m/mwt. To homogenize the suspensions, each mixture was sonicated at 50 KJ/g CNC using a Hielscher UP400st ultrasonic processor with a 3 mm diameter titanium tip operating at 24 KHz, 80% amplitude, and 80% capacity. 372,5  $\mu\text{L}$  of lactic acid 0.1M and 1g of chitosan 2% m/m were then added to each mixture and dissolved using magnetic stirrers. After the chitosan dissolved completely, each mixture was left to rest for at least 20 minutes at 4 degrees Celsius. A solution of  $\beta$ -GP 50% m/v and millipore ultrapure water was prepared and chilled at 4 degrees Celsius. This solution was then added to the mixture dropwise with

agitation with concentrations of 5%, 6.25% and 8.66% m/m for each concentration of CNC as seen in table xx and placed in the fridge to rest.

For the composites with a 3.5% CNC concentration, the 4.5% suspension of CNC previously prepared was used instead of the original solution. This slight change in concentration and procedure was to remove the need to add water therefore sonication was no longer necessary. All other steps were kept the same.

### 3.4 Hydrogels Production

To obtain hydrogels with the desired shapes, a 3D printed mold with cylindrical holes was used to confine the mixture previously prepared. Each mixture was placed in a small syringe and centrifuged using a Thermo Scientific Multifuge X1R Refrigerated Centrifuge at 2000 rpm and 20 degrees Celsius, in increments of 3 minutes until all the air bubbles were removed. The mixture was then injected in each slot of the mold and placed in an incubator at 37 degrees Celsius with a saturated atmosphere. The gelation time for each of the mixtures was different and they were only removed from the molds once these became firm without occurring fractures. The specific time for each Sample can be seen in Table 3.1.

Table 3.1: Composition and gelation times of each composite mixture

|    | Concentration wt.% |     |     |      | Gelation Time |  |
|----|--------------------|-----|-----|------|---------------|--|
|    | CS                 | CNC | AL  | GP   |               |  |
| 2A | 1                  | 2   | 0.9 | 8.66 | 1h            |  |
| 2B |                    |     |     | 6.25 | 2h30min       |  |
| 2C |                    | 3   |     | 5    | 3h            |  |
| 3A |                    |     |     | 8.66 | 40min         |  |
| 3B |                    | 3   |     | 6.25 | 1h            |  |
| 3C |                    |     |     | 5    | 2h30min       |  |

### 3.5 Rheology Tests

For these tests a MCR 502 Rotational Rheometer (Anton Paar, Austria) with a parallel plate geometry of 25 mm and a 1 mm gap was used. To perform oscillatory tests, such as temperature sweep tests, it was necessary to first determine the limits of the linear viscoelastic region (LVR). The limits determined were an angular frequency of 1 Hz and a shear strain of 10%.

#### 3.5.1 Temperature Sweep Test and Viscosity

To analyze the elastic modulus ( $G'$ ) and viscous modulus ( $G''$ ) within the linear regime, the temperature was elevated at a rate of  $2^{\circ}\text{C}/\text{min}$  from  $20^{\circ}\text{C}$  to  $60^{\circ}\text{C}$ . The gelation

temperature was determined to be when  $G' = G''$ , the sol-gel transition point. This is because if  $G' < G''$ , the sample is in a solution state and if  $G' > G''$ , the sample is in a gel state.

Viscosity tests allow conclusions to be drawn regarding the formulation's behavior under varying shear rates. The tests were performed at 20°C, with the shear rate increasing exponentially from 0.08 to 1000 s<sup>-1</sup>.

### 3.6 Unconfined & Confined Compression Tests

A universal testing Rheometric Scientific (*Minimat Firmware Version 3.1*) machine was used with an atmosphere of 37°C for the unconfined compression tests. The diameter and height of each sample were determined using a digital caliper. Each sample was compressed to a maximum load of 19N at a velocity of 0.2 mm/min. Five tests were performed for each sample.

For the confined compressions tests the equipment had to be modified with new clamps to fit the necessary configurations. The compression system, specifically designed for these tests, has to be installed and aligned. As with the previous test, the diameter and height were measured and then placed in the test interface, in this case, within the confined water bath.

## RESULTS AND DISCUSSION

### 4.1 Designing the Compression System

For the confined compression tests, a new system had to be designed to fit the necessary criteria. This would have to consist of a baseplate, to confine the hydrogel and keep it in a water bath, and an arm, to compress the hydrogel. After designing these in CAD using SolidWorks, and modifying it to fit the needs, described in Appendix A, the final models seen in Figure 4.1-(a)(b) were sent to be printed in PLA.

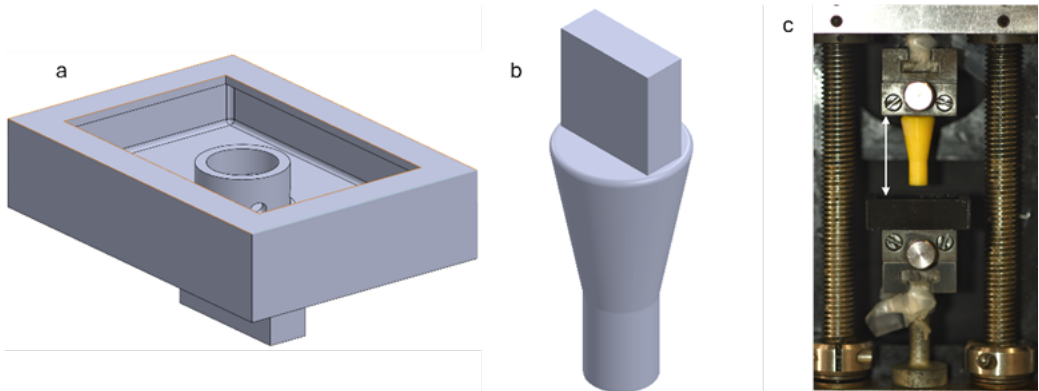


Figure 4.1: (a) Final base CAD design; (b) Final arm CAD design; (c) Printed compression system mounted in the universal testing

To correctly attach both pieces to the Compression test machine required perfect alignment with each other. This proved to be a very challenging step as the slightest misalignment would cause a lot of noise in the data gathered. This was likely due to the rough finish of the pieces causing friction causing huge spikes in the stress/strain curves. This issue was greatly minimized after the surface of the pieces was smoothed using acetone. While not the best option, rubbing small amounts of acetone on the test interfaces degrades the surface finish left from the printer making both prints smoother. This primarily impacted the alignment time as less adjustment was required to remove the noise. The attached system can be seen in Figure 4.1-(c).

## 4.2 Rheology Tests

### 4.2.1 Temperature Sweep Test

The addition of CNCs was expected to lower the gelation temperature as its concentration increased to 37°C or lower. This would also be expected as the concentrations of the cross-link agent, GP, Increased. These results are to be expected according to research found [16] [17]

In the graph below (Figure 4.2) we can observe these effects and compare them. The gelation temperatures decreased as expected as the GP concentration Increased, even by just a small increment, as did for the CNC concentrations, with the only exception of sample 5/CNC3 where the temperature had a slight Increase. The samples 5/CNC4, 6CNC3, 6CNC4, 9CNC3 and 9CNC4, had already passed the sol-jell therefore the exact temperature could not be determined. The expected decrease in temperatures was similar, although it had a steeper decrease in temperatures than what was observed.

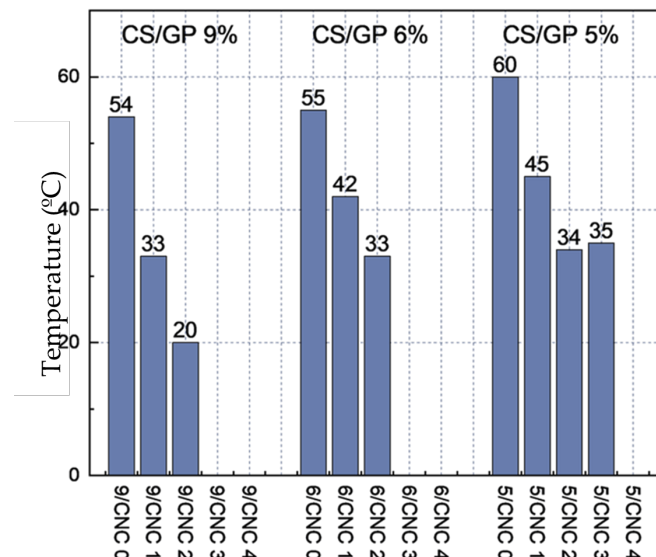


Figure 4.2: Summary of the gelation temperatures obtained from the temperature sweep tests

For the desired application of this hydrogel, it was determined that the ideal samples to continue testing would be the mixtures 2% and 3% CNC with 5%, 6% and 9% GP. These were chosen due to their gelation temperatures being within a range of 20°C to 37°C, and having a higher concentration of CNC, meaning higher reinforcement.

### 4.2.2 Viscosity

The viscosity curves shown in Figure 4.3 suggest non-Newtonian behavior, where viscosity decreases as the shear rate increases, demonstrating shear-thinning [16]. There does not seem to be a correlation between the increase in GP content and the increase in viscosity, in the range of GP used, and the increase in CNC concentration cannot be concluded either.

Although we can conclude that the addition of CNC does not affect the viscous behavior at 20°C due to the range of values obtained being very similar. All viscosity curves seem to present three different regions where the slope is different, resembling the behavior of polymer liquid crystals as the aqueous liquid crystalline CNC suspensions.

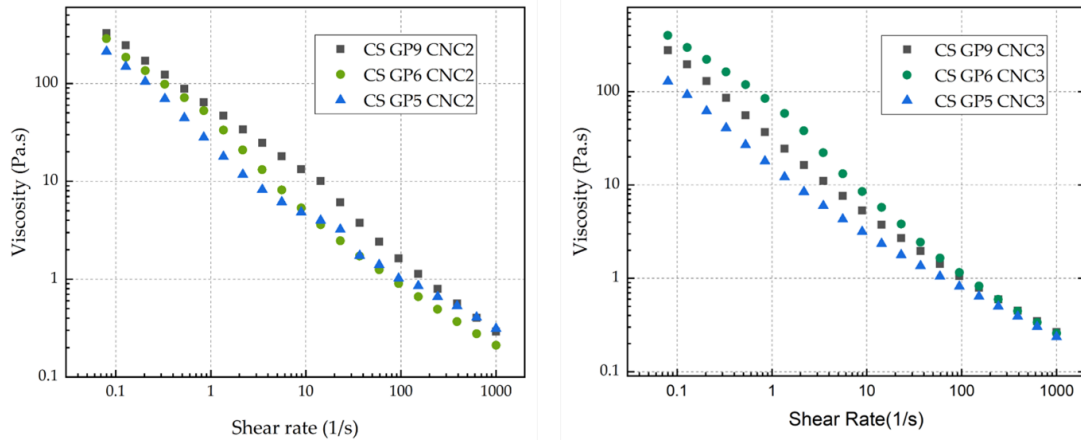


Figure 4.3: Summary graph of the viscosity curves as a function of the shear rate for the 2% & 3% CNC samples series at 20°C

### 4.3 Preparing Hydrogels

22 mL syringes were filled with each mixture and centrifuged until all air bubbles were removed. These were then injected into the molds withing a petri dish. To prepare firm hydrogels in these molds with no fractures once removed It was necessary to saturate the Incubator at 37°C with water to create an 80% humidity atmosphere to let the hydrogels form without water loss. The gelation times used for each mixture are shown in Table 3.1.

After leaving the samples in the Incubator for the times referred, they were carefully removed from the molds and rinsed before being placed in a flask with water at 37°C and stored in the Incubator at 37°C until used. The result of the formed hydrogels can be seen in Figure 4.4. Due to the high viscosity of the mixtures, some imperfections in the structure can be seen.



Figure 4.4: Perspective a) top view and b) front view of a CS/GP9%/CNC2% hydrogel, with a scale bar of 5 mm.

## 4.4 Compression Tests

The hydrogels were characterized based on their mechanical properties under confined and unconfined compression. For the unconfined tests, a semi-closed environment was prepared around the equipment to control the temperature during each test. For the confined tests this was not possible due to the more complex system being used. To minimize temperature loss as much as possible, the hydrogels and water were only removed from the incubator when the equipment was fully prepared to start a new test. When preparing the sample, its diameter and height were measured using a digital caliper. Then, it was placed on the base plate or inside the base chamber for the respective tests, and water was added to the system in the confined tests. For each test a force/displacement graph was obtained, and with this a stress/strain graph was produced. For this the stress and strain were found using the following equations:

$$\text{stress} = \frac{\text{force}}{\text{area}} \quad \text{strain} = \frac{\text{displacement}}{\text{initial height}}$$

From these graphs we can find the Young's module for the unconfined tests and the aggregate modulus for the confined tests by measuring the slope of the Initial linear section (ILS). The aggregate modulus measures the stiffness of tissue at equilibrium after all fluid flow has stopped. A higher aggregate modulus indicates that the tissue deforms less under a given load. [18]

### 4.4.1 Unconfined Tests

According to other studies, the Increase in CNC concentration should promote an Increase of the Young's modulus, due to Improved mechanical properties [19]. The first compression tests done were unconfined, meaning there was no restriction to their movement when under load. The graph represented in Figure 4.5, is an example of a stress/strain graph obtained from the unconfined tests.

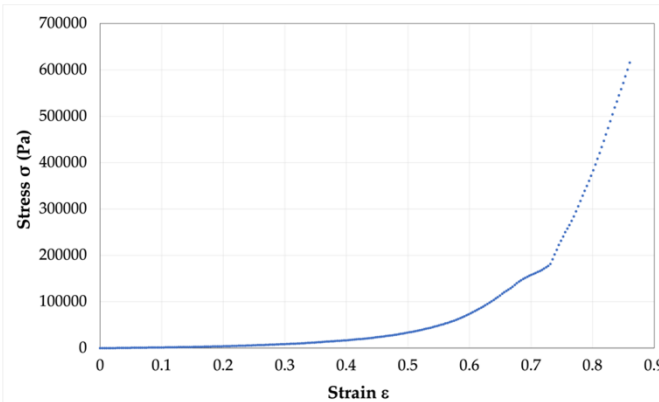


Figure 4.5: Stress/strain curve obtained from a compression test of the CS/GP9%/CNC3% sample

The Young's modulus is obtained from the linear region of the beginning of the curve.

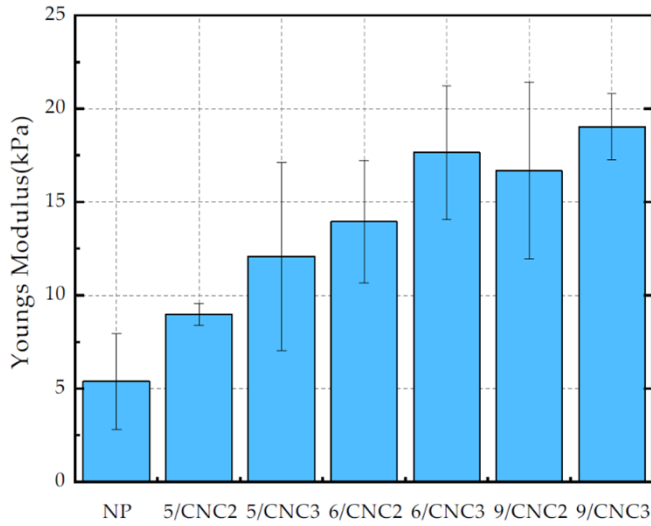


Figure 4.6: Histogram of the Young's moduli obtained at 37°C, with n=5

In Figure 4.6 it can be seen the summary of all unconfined test performed to all 6 samples. We can see a clear increase in the Young's modulus with the increase in CNC concentration. These can also be compared to the Young's modulus of a healthy Human NP. This effect is due to the increase in hydrogen bonds within the CS and CNC chains [19]. Along with the increase of CNCs, it can also be observed how the increase in GP concentration also promotes an increase in the Young's modulus, likely due to denser crosslinking.

#### 4.4.2 Confined Tests

As mentioned before, once the samples were measured, they were placed within the compression chamber seen in figure (section 4.1c) and the arm was lowered. This became the first problem faced. since the sample Is completely covered by the arm there was no way to determine when the compression arm had reached the sample. The solution used was to lower the arm and once a resistance was recorded the respective displacement would be recorded as the beginning of the compression phase.

In Figure 4.7-(a)(b) a change in behavior can be seen that was not expected. Once it reaches higher stress values this effect seems to be less noticeable. A different result but also unexpected was then recorded as seen in Figure 4.7-(c)(d) where the repeating small spikes in stress are replaced with two larger spikes. after analyzing these results and the compression system carefully It was determined that these spikes were a result of friction and misalignment of the two pieces. due to the pieces being 3d printed, the rough finish proved to be enough to be felt by the equipment when not perfectly aligned.

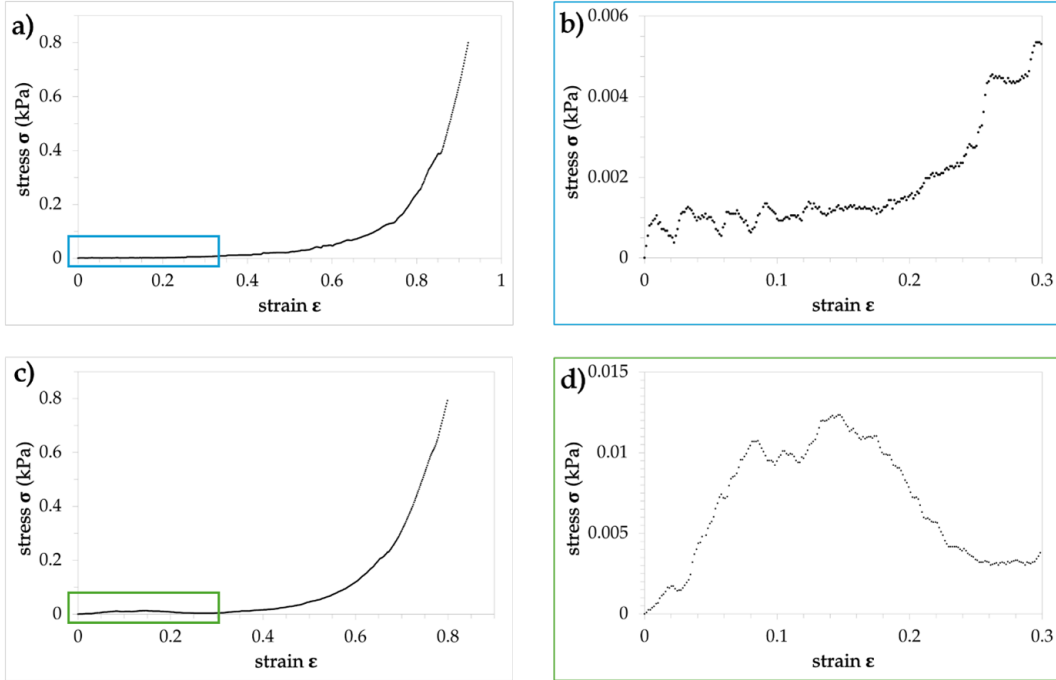


Figure 4.7: First results from confined compression tests with high noise with sample 2CS/2CNC/9GP: a) First full compression; b) Initial section of image a; c) Seventh full compression; d) Initial section of Image c

To remove the effect of the friction, acetone was used to slightly degrade the surface of both pieces in their interfaces. Due to PLA's high density, it would ideally not affect the structure of the pieces but slightly smoothen the surface therefore improving the movement of the interface and improve the alignment. Along with the surface treatment, the method to determine first contact with the hydrogel within the chamber was altered. The distance between two points in the system displayed in Figure 4.1-(c) was measured when the arm reached the very top of the chamber. since the depth of the chamber is known to be 5 mm and the height of the hydrogel was measured. the distance the arm must be lowered until coming in contact with the sample can then be calculated. In Figure 4.8-(a)(b) we can see the result of these improvements. the tests performed had two phases, an initial 20% compression, followed by 10 minutes of relaxation and then compressed 100%. the noise was not completely removed but greatly improved and both 20% compressions and 100% compressions tended to follow a similar path. With these results we could measure the aggregate modulus for both tests as seen in Figure 4.8-(c)(d). the aggregate modulus for the 20% compression was 306 kPa and 301.5 kPa for the 100% compression. these results were very similar, meaning the hydrogel regain most of its Initial structure during the relaxation period. these values were 20 times the results for the Young's modulus of the unconfined tests for the same sample, but only 50% of the aggregate modulus of a healthy NP. [20]

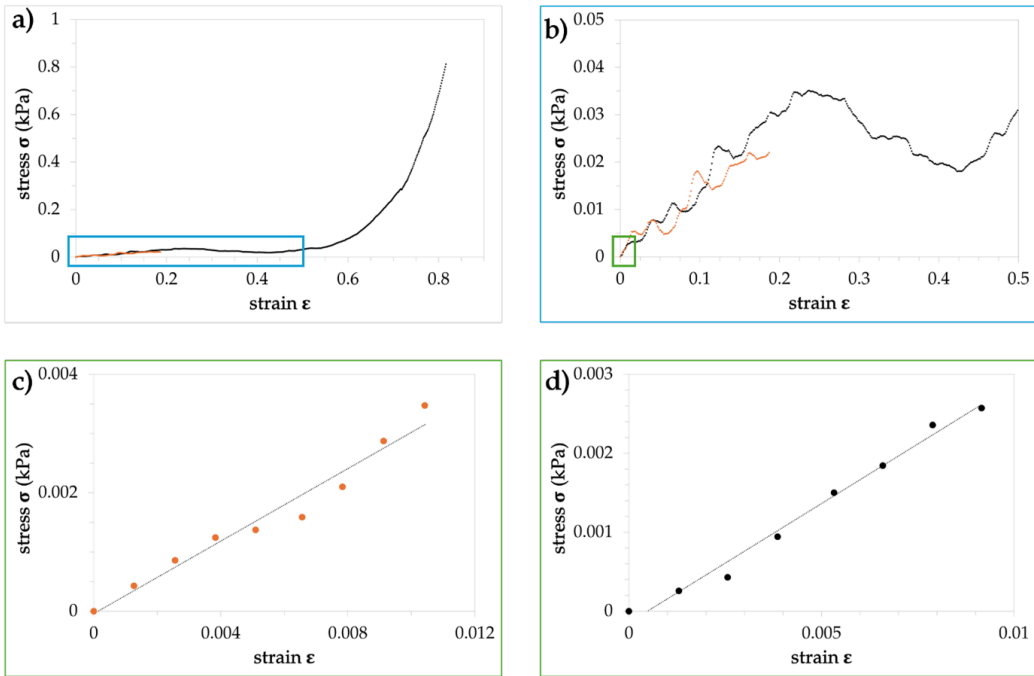


Figure 4.8: Results of compression tests with sample 2CS/2CNC/9GP after surface treatment as done to the system: a) 20% compression (orange) and 100% compression (black); b) Section of image a; c) ILR for the 20% compression test; d) ILR for the 100% compression test

There weren't many results like this one, not enough to be able to take conclusions on the behavior of the hydrogels in confined compressions tests. Figure 4.9-(a) shows an example of a test where a new behavior was seen. From Figure 4.9-(b), we can see the inconsistency in data point, especially in the initial section of the test. This made the determination of the aggregate modulus very difficult due to there not being a very good ILS (Figure 4.9-(c)(d)). The modulus' determined were both around 20 kPa, much closer to the Young's modulus determined than to the previously shown aggregate modulus. After multiple tests with very similar results the equipment was removed, cleaned and analyzed. The chamber did not show any signs of deformation but did show a lot of accumulation of possible residue from previous tests. It is possible that due to the surface treatment and general wear from all the tests degraded the pieces enough to cause these affect to the results.

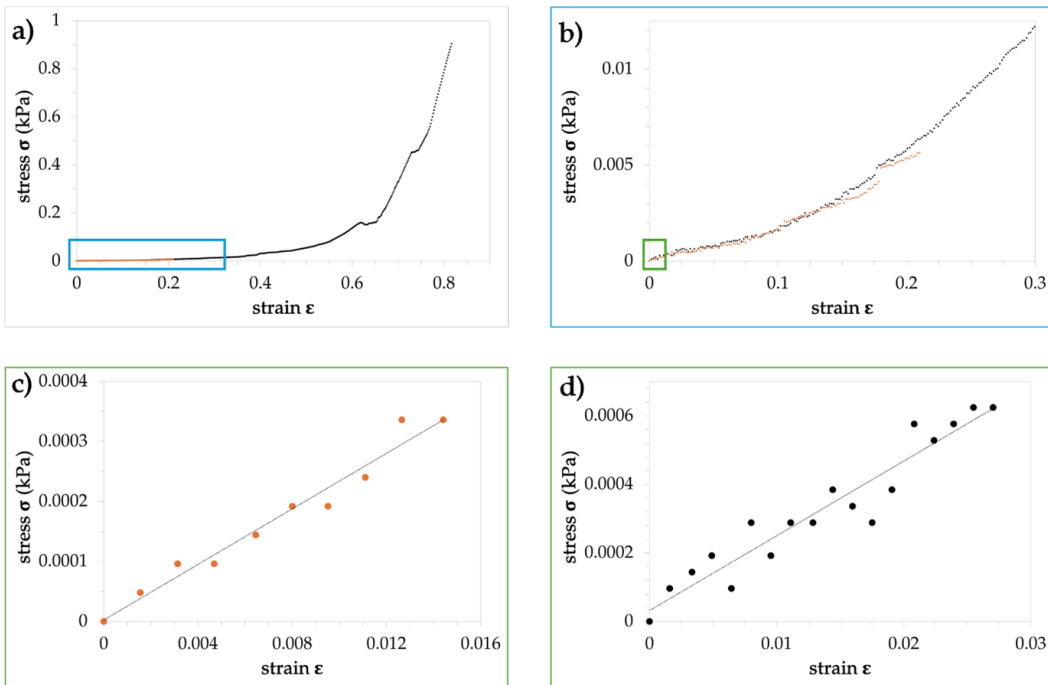


Figure 4.9: Results of the last compression tests with sample 2CS/2CNC/9GP: a) 20% compression (orange) and 100% compression (black); b) Section of image a; c) ILR for the 20% compression test; d) ILR for the 100% compression test

Although PLA has a much higher Young's modulus than the NP and seemed to be a good material choice for the compression pieces, these results show that not only 3D-printed PLA leaves too rough of a surface for these applications, but it does not last as long as it was expected Figure 4.10. In future works, it is suggested to produce several bases, treat them with acetone and use them in a few numbers of tests. A transparent material should also be advisable as assessing the beginning of the position of the arm is of paramount importance to be able to perform the type of tests described above: first cycle to 20% of compression, followed by uncompressing and relaxation and full compression.



Figure 4.10: Confined compression base after 20 tests were performed and cleaned

## 4.5 Additional Tests

A small mixture of 8.4g CNC 4.5% (Appendix 2) and 74.5  $\mu$ L of lactic acid was prepared to see if these liquid crystalline phases would still form after mixed and left to rest. Although

isotropic-anisotropic phase separation was not visible due to the solution becoming viscose, when placed between crossed polarizers birefringence could be observed evidence of the liquid crystalline phase — Figure 4.11.

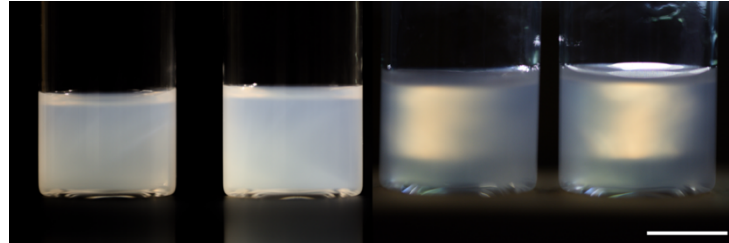
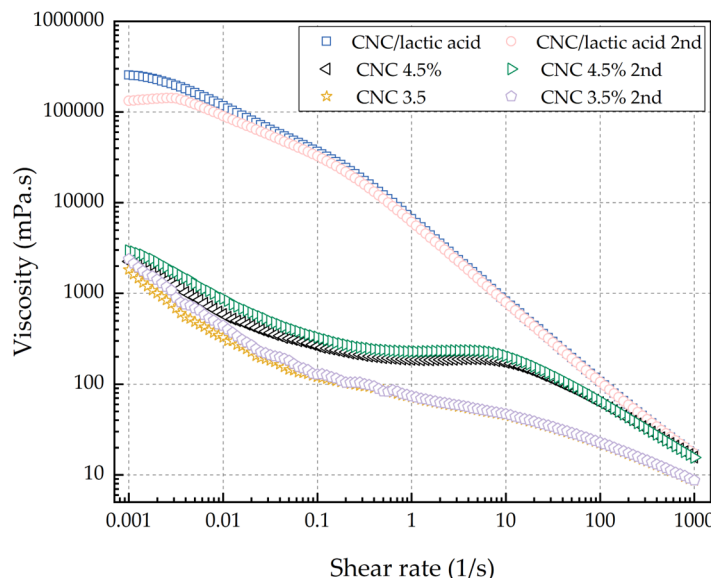


Figure 4.11: Birefringence effect observed when sample is seen between crossed polarizers, with a scale bar of 13.7 mm.

Viscosity curves of CNC suspensions and CNC with acid lactic were obtained in order to infer on the behavior of these suspensions under shear figure A.1). It is possible to see in both CNC suspension flow curves the presence of three regions of different slopes characteristic of their liquid crystalline behavior, being more pronounced at the suspension with higher CNC [21]. At low shear rates, the cholesteric LC domains aligned, inducing shear-thinning. At intermediate shear rates, the suspension behaves almost like a Newtonian fluid and a plateau-like regime is observed where all the LC domains are aligned. If the LC domains are partly aligned in this region, a less evident than that of the first region shear-thinning is observed. At higher shear rates, the LC domains are destroyed, and the orientation of the nanoparticles with the shear direction will occur, inducing further shear-thinning. Adding acid lactic to the suspension of CNC with a nanoparticle content of 4.5 wt.% greatly increases the viscosity of the suspension observed at low shear rates. Although the obtained flow curve does not follow the observed for pristine CNC, one can still observe three different regimes in the shear-thinning as the shear rate increases.



## CHAPTER 4. RESULTS AND DISCUSSION

Figure 4.12: Viscosity as a function of shear rate for aqueous suspensions of CNC with 3.5 and 4.5 wt.% and CNC (4.5 wt.%) with acid lactic. Duplicates are shown to highlight test accuracy

## CONCLUSIONS

This project aimed to propose a minimally invasive method for treating IDD by developing an injectable CNC-reinforced hydrogel. The proposed hydrogel formulation included chitosan as the matrix, CNCs as the reinforcement, GP as the crosslinking agent, and lactic acid as the acidic medium. This formulation was chosen to design a hydrogel capable of withstanding the loads typically experienced by the NP, restoring its functions and structure. For this, rheology tests and compression tests were performed. For the purpose of this hydrogel, it was important that the transition sol/gel would be between 20°C and body temperature, so 37°C. With this, it was determined that samples with 2% and 3% CNC showed the most promising gelation result. With the initial unconfined tests, an improvement of mechanical properties could be observed with the increase in CNC concentration, showing Young's modulus ranging from 9 to 19kPa. Comparing these results to the modulus of a healthy NP from other studies, we can conclude that these hydrogels could support loads typically felt by the NP. A major part of this project was to develop a confined compression test system to simulate the disc. The tested interface printed in PLA proved not to be an ideal interface, due to the rough surface finish and placement difficulties. Along with the complications of calculating the beginning of each test, the pieces deteriorated quickly. With these difficulties, not enough data was retrieved to be able to evaluate the aggregate modulus of the prepared hydrogels. The LC suspensions showed very distinct flow regions. these results could be very valuable If combined with the formulation already tested, possibly Improving the mechanical properties even more.

In summary, the development of an injectable thermosensitive chitosan-based hydrogel reinforced with CNCs was successful. Both rheological and Young's modulus results showed this system to be a possible solution to helping with IDD and with regeneration of the NP. A major limitation in this project was the choice of material for the confined system. PLA proved to be an inefficient choice for this application due to its roughness during tests, lasting only a few tests, and limiting view of the sample during the tests. Improving this system, primarily looking for a more suitable material, ideally transparent, would greatly improve preparations for testing as well as the results. A possible solution

## CHAPTER 5. CONCLUSIONS

---

to the strength would be to print multiple pieces and change pieces more frequently. This is necessary to continue evaluating the mechanical properties of the hydrogel developed. Adapting the formulation with the LC suspensions tested could also be of interest to this study.

## BIBLIOGRAPHY

- [1] J. M. Lourenço. *The NOVAtesis L<sup>A</sup>T<sub>E</sub>X Template User's Manual*. NOVA University Lisbon. 2021. URL: <https://github.com/joaomlourenco/novathesis/raw/main/template.pdf> (cit. on p. i).
- [2] B. Innocenti and F. Galbusera. "Human Orthopaedic Biomechanics Fundamentals, Devices and Applications". In: London: Academic Press, 2022. Chap. 11. DOI: [10.1016/C2020-0-01750-0](https://doi.org/10.1016/C2020-0-01750-0) (cit. on p. 1).
- [3] E. C. Benzel. "Biomechanics of the Spine Stabilization". In: 3rd. New York: Thieme Medical Publishers, 2015. Chap. 4. DOI: [10.1055/b-0035-106378](https://doi.org/10.1055/b-0035-106378) (cit. on p. 1).
- [4] M. Nordin and V. H. Frankel. "Basic Biomechanics of the Musculoskeletal System". In: 3rd. Philadelphia: Lippincott Williams & Wilkins, 2001. Chap. 10. DOI: [10.1016/S0021-9290](https://doi.org/10.1016/S0021-9290) (cit. on p. 1).
- [5] M. A. Adams and P. J. Roughley. "What is Intervertebral Disc Degeneration and What Causes It?" In: *Spine* 31.18 (2006), pp. 2151–2161. DOI: [10.1097/01.brs.0000231761.73859.2c](https://doi.org/10.1097/01.brs.0000231761.73859.2c) (cit. on p. 1).
- [6] F. Galbusera et al. "Cervical Spine Biomechanics following Implantation of a Disc Prosthesis". In: *Medical Engineering & Physics* 30.9 (2008), pp. 1127–1133 (cit. on p. 2).
- [7] C. Yan et al. "Applications of Functionalized Hydrogels in the Regeneration of the Intervertebral Disc". In: *BioMed Research International* 2021.1 (2021). DOI: [10.1155/2021/2818624](https://doi.org/10.1155/2021/2818624) (cit. on pp. 2, 4).
- [8] P. Rahamanian-Devin, V. B. Rahimi, and V. R. Askari. "Thermosensitive Chitosan- $\beta$ -Glycerophosphate Hydrogels as Targeted Drug Delivery Systems: An Overview on Preparation and Their Applications". In: *Advances in Pharmacological and Pharmaceutical Sciences* 2021.1 (2021), pp. 1–17. DOI: [10.1155/2021/6640893](https://doi.org/10.1155/2021/6640893) (cit. on pp. 2, 5).
- [9] P. Maturavongsadit et al. "Cell-Laden Nanocellulose/Chitosan-Based Bioinks for 3D Bioprinting and Enhanced Osteogenic Cell Differentiation". In: *ACS Applied Bio Materials* 4.3 (2021), pp. 2342–2353 (cit. on p. 3).

## BIBLIOGRAPHY

---

- [10] J. You et al. "Rheological Study of Physical Cross-Linked Quaternized Cellulose Hydrogels Induced by  $\beta$ -Glycerophosphate". In: *Langmuir* 28.11 (2012), pp. 4965–4973. doi: [10.1021/la2046417](https://doi.org/10.1021/la2046417) (cit. on p. 3).
- [11] C. Rodrigues et al. "Production and Application of Lactic Acid". In: *Current Developments in Biotechnology and Bioengineering: Production, Isolation and Purification of Industrial Products* (2016), pp. 543–556. doi: [10.1016/B978-0-444-63662-1.00024-5](https://doi.org/10.1016/B978-0-444-63662-1.00024-5) (cit. on p. 3).
- [12] R. R. da Rosa et al. "Cellulose and Chitin Twisted Structures: From Nature to Applications". In: *Adv. Funct. Mater* (2023). doi: [10.1002/adfm.202304286](https://doi.org/10.1002/adfm.202304286) (cit. on p. 3).
- [13] P. Maturavongsadit et al. "Thermo-/pH-responsive chitosan-cellulose Nanocrystals Based Hydrogel with Tunable Mechanical Properties for Tissue Regeneration Applications". In: *Materialia* 12 (2020). doi: [10.1016/j.mtla.2020.100681](https://doi.org/10.1016/j.mtla.2020.100681) (cit. on pp. 4, 5).
- [14] A. E. Kommos et al. "Development of Improved Confined Compression Testing Setups for Use in Stress Relaxation Testing of Viscoelastic Biomaterials". In: *Gels* 10.5 (2024), p. 329. doi: [10.3390/gels10050329](https://doi.org/10.3390/gels10050329) (cit. on pp. 4, 5).
- [15] H. Qin et al. "Preparation and Characterization of Chitosan/ $\beta$ -Glycerophosphate Thermal-Sensitive Hydrogel Reinforced by Graphene Oxide". In: *Frontiers in Chemistry* 6.565 (2018). doi: [10.3389/fchem.2018.00565](https://doi.org/10.3389/fchem.2018.00565) (cit. on p. 5).
- [16] H. Xu et al. "Enhanced cutaneous wound healing by functional injectable thermo-sensitive chitosan-based hydrogel encapsulated human umbilical cord-mesenchymal stem cells". In: *International Journal of Biological Macromolecules* 137 (2019), pp. 433–441. doi: [10.1016/j.ijbiomac.2019.06.246](https://doi.org/10.1016/j.ijbiomac.2019.06.246) (cit. on p. 10).
- [17] S. Kempe et al. "Characterization of thermosensitive chitosan-based hydrogels by rheology and electron paramagnetic resonance spectroscopy". In: *European Journal of Pharmaceutics and Biopharmaceutics* 68.1 (2008), pp. 26–33. doi: [10.1016/j.ejpb.2007.05.020](https://doi.org/10.1016/j.ejpb.2007.05.020) (cit. on p. 10).
- [18] J. M. Mansour. "Biomechanics of Cartilage". In: *Kinesiology: The Mechanics and Pathomechanics of Human Movement 2nd Edition*. Ed. by C. A. Oatis. Baltimore, MD, USA: Wolters Kluwer, 2003. Chap. 5, pp. 69–83 (cit. on p. 12).
- [19] C.-z. Geng et al. "Mechanically Reinforced Chitosan/Cellulose Nanocrystals Composites with Good Transparency and Biocompatibility". In: *Chinese Journal of Polymer Science* 33 (2015), pp. 61–69. doi: [10.1007/s10118-015-1558-6](https://doi.org/10.1007/s10118-015-1558-6) (cit. on pp. 12, 13).
- [20] W. Johannessen and D. M. Elliott. "Effects of degeneration on the biphasic material properties of human nucleus pulposus in confined compression". In: *Spine* 30.24 (2005), E724–E729. doi: [10.1097/01.brs.0000192236.92867.15](https://doi.org/10.1097/01.brs.0000192236.92867.15) (cit. on p. 14).

- [21] C. Qiao et al. "Structure and rheological properties of cellulose nanocrystals suspension". In: *Food Hydrocolloids* 55 (2016), pp. 19–25. DOI: [10.1016/j.foodhyd.2015.11.005](https://doi.org/10.1016/j.foodhyd.2015.11.005) (cit. on p. 17).

# A

## DEVELOPMENT OF THE COMPRESSION SYSTEM

Both pieces had to be modified multiple times, each model was to test specific conditions desired for the tests. The compression arm did not require many modifications as it only needed to be adjusted if the interface on the base plate was modified. On the other hand, the base plate had multiple modifications. The infograph in Figure A.1 shows the progression of the design.

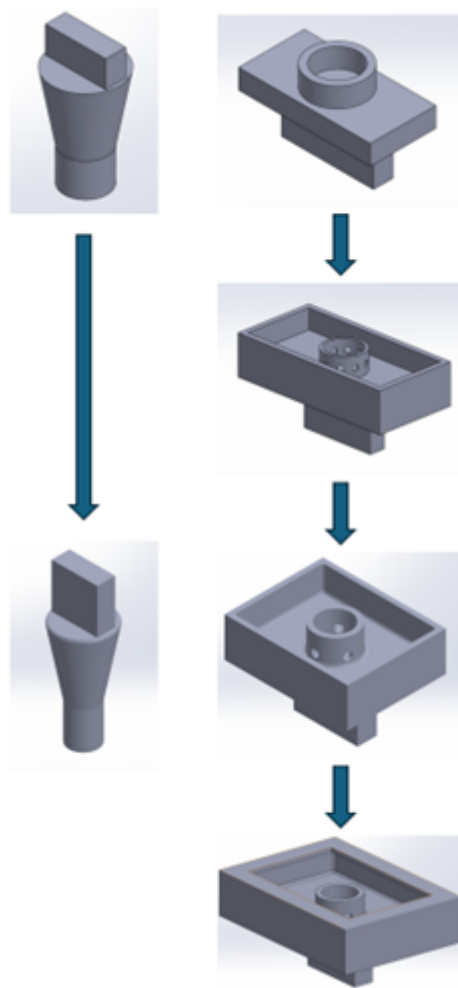


Figure A.1: Progress of compression system development.

The first two models were a very simple concept that fit the main criteria, confine a sample and compress it. The next modification was to the base where walls were added to add water and holes were made in the chamber to let the samples expel and absorb water. Following that change these were placed on the equipment to test fit. The first change to be made was the anchor points for the clamps were extended to increase the area of contact with both clamps. The height of the base plate was also extended from 4mm to 5mm to add some margin for the samples. The final change was to the base plate where the exterior walls were extended slightly above the chamber walls and was extended inward to avoid water splashing on the equipment.

# B

## CNC SUSPENSION 4.5% AND GRAVIMETRIC ANALYSIS

A large quantity of CNC 4.5% suspension was prepared in two different flasks to be used for additional tests. The main objective of this dilution and filtration was to get a CNC suspension with a lower concentration and visible Crystalline Cholesteric Phases. To determine the real concentration of the suspensions, 7 small samples from each flask were placed on separate eppendorf tubes and weighed. Once done, they were placed in the oven at 60°C and weighed twice a day until the results stabilized. After reviewing the results, it was determined the suspensions had concentrations of 4.76% and 4.63% — see Figure B.1.

Table B.1: Gravimetric analysis of the CNC 4.5% suspension

|    |   |        | 28/02 (11:00)  | 28/02 (18:30)        | 29/02 (10:30) | 29/02 (18:30) | 01/03 (11:00) |        |        |              |            |                      |
|----|---|--------|----------------|----------------------|---------------|---------------|---------------|--------|--------|--------------|------------|----------------------|
|    |   |        | M. Expend. (g) | M. Expend.+susp. (g) | 1             | 2             | 3             | 4      | 5      | M. Susp. (g) | M. CNC (g) | Concentração CNC (%) |
| C1 | A | 0.477  | 0.5319         | 0.4798               | 0.4794        | 0.4799        | 0.4795        | 0.4796 | 0.0549 | 0.0026       | 4.7359     |                      |
|    | B | 0.4714 | 0.5159         | 0.4736               | 0.4736        | 0.4735        | 0.4737        | 0.4735 | 0.0445 | 0.0021       | 4.7191     |                      |
|    | C | 0.4598 | 0.5024         | 0.4621               | 0.462         | 0.4618        | 0.4619        | 0.4619 | 0.0426 | 0.0021       | 4.9296     |                      |
|    | D | 0.4574 | 0.5001         | 0.4595               | 0.4595        | 0.4595        | 0.4595        | 0.4595 | 0.0427 | 0.0021       | 4.918      |                      |
|    | E | 0.4631 | 0.503          | 0.4651               | 0.4651        | 0.4653        | 0.4651        | 0.4651 | 0.0399 | 0.002        | 5.0125     |                      |
|    | F | 0.4618 | 0.5074         | 0.4639               | 0.4639        | 0.4642        | 0.4644        | 0.4639 | 0.0456 | 0.0021       | 4.6053     |                      |
|    | G | 0.4687 | 0.5549         | 0.4725               | 0.4725        | 0.4725        | 0.4725        | 0.4725 | 0.0862 | 0.0038       | 4.4089     |                      |
|    |   |        |                |                      |               |               |               |        |        |              |            | Avg. 4.76%           |
| C2 | A | 0.387  | 0.43           | 0.3893               | 0.389         | 0.389         | 0.3888        | 0.3888 | 0.043  | 0.0018       | 4.186      |                      |
|    | B | 0.463  | 0.5055         | 0.465                | 0.4649        | 0.4648        | 0.4647        | 0.4648 | 0.0435 | 0.0018       | 4.1379     |                      |
|    | C | 0.4674 | 0.5066         | 0.4693               | 0.4694        | 0.4694        | 0.4694        | 0.4694 | 0.0392 | 0.002        | 5.102      |                      |
|    | D | 0.466  | 0.5127         | 0.4682               | 0.4683        | 0.4682        | 0.4682        | 0.4682 | 0.0467 | 0.0022       | 4.7109     |                      |
|    | E | 0.4622 | 0.5063         | 0.4643               | 0.4641        | 0.4642        | 0.4644        | 0.4644 | 0.0441 | 0.0022       | 4.9887     |                      |
|    | F | 0.4713 | 0.5161         | 0.4734               | 0.4733        | 0.4734        | 0.4734        | 0.4734 | 0.0448 | 0.0021       | 4.6875     |                      |
|    | G | 0.4597 | 0.5077         | 0.462                | 0.4619        | 0.4619        | 0.4619        | 0.4619 | 0.048  | 0.0022       | 4.5833     |                      |
|    |   |        |                |                      |               |               |               |        |        |              |            | Avg. 4.63%           |



# Hydrogels for load support in the nucleus pulposus of intervertebral discs

## Eduardo 2024